

# LOCAL DAMAGES AND MATERIALS DURABILITY PROGNOSTICATION FOR HIGH PARAMETERS MEDIUM

B.A. KHADYRBEKOV, V.N. PECHERSKY  
and V.V. BORISEVITCH

*Kazakh Chemical Technology Institute, Tauke-khan Avn.,  
5, Shimkent-18, Republic of Kazakhstan, SU (CIS)*

P.A. PAVLOV

*St. Petersburg State Technical University,  
Politekhnikeskaya Str., 29, St. Petersburg, Russia, CIS(US)*

## ABSTRACT

We propose a number of equations to evaluate the service life of materials in corrosive media. We analyzed several cases: uniform stress corrosion, stress corrosion cracking and corrosion cracking with low-rate deformation, low-cycle corrosion fatigue. The analysis results for the stated above corrosion-mechanical injuries are also given in the paper.

## KEYWORDS

Stress corrosion, stress corrosion cracking, low-cycle fatigue. Discussions and Results  
The authors propose several variants of injuries mathematical models based on the kinetic approach and experimentally tested on their usage efficiency. In case of corrosion cracking while operating the material and under the influence of corrosion medium we propose the following force-type kinetic equations for the stage of scattered injuries:

$$d\eta/d\tau = f[\sigma(\tau); \dot{\sigma}(\tau); T(\tau); \eta(\tau); C(\tau)] \quad (1)$$

where  $\eta$  - some injury measure within  $0 < \eta < 1$ ;  $\sigma(\tau)$  - loading regime;  $\dot{\sigma}(\tau)$  - loading rate;  $T(\tau)$  - temperature defined at function of time;  $C(\tau)$  - a parameter taking into account the character of the aggressive medium influence on the metal deformed. The equality  $\eta = 0$  corresponds to the undamaged material and the equality  $\eta = 1$  is the injury condition. In the simplest case the injury  $\eta$  can depend only on the level of acting stresses and the solution of the differential equation (1) leads to the formula of the linear injury summation:

$$= \int_0^{\tau} d\theta / t[\sigma(\theta)] \quad (2)$$

Kinetic equations of non-linear injury summation possess great opportunities. Let us introduce an independent time parameter as well as stress parameter  $\sigma$  into the equation;

$$d\Pi/d\tau = f(\sigma, \tau) \quad (3)$$

Having taken time function in the form of power dependence  $A\tau^m$  we get:

$$\Pi = \int_0^{\tau} \frac{m \cdot \theta^{m-1}}{t^m [\sigma(\theta)]} d\theta \quad (4)$$

Having taken time function in the form of exponential dependence  $Ae^{r\tau}$  we get:

$$\Pi = r \int_0^{\tau} e^{r[\theta - t[\sigma(\theta)]]} d\theta \quad (5)$$

The constants  $m$  and  $r$  defined from the conditions of the experimental data best description under non-stationary loading regimes are introduced to the dependences (4) and (5).

The dependences (4) and (5) modifications are as follows:

$$\Pi = \sum_{k=1}^n (\tau_k / t_k)^m \quad (5^*)$$

$$\Pi = \sum_{k=1}^n e^{r(\tau_k - t_k)} \quad (6)$$

We can also use the well-known injury equation:

$$d\Pi/d\tau = \psi (d\sigma/d\tau) + f(\sigma) \quad (7)$$

whence it follows:

$$\Pi = \sigma(\tau) / \sigma_p + \int_0^{\tau} \frac{1 - \sigma_\theta / \sigma_p}{t[\sigma(\theta)]} d\theta \quad (8)$$

The efficiency experimental test of this or that kinetic equation was conducted on the basis of two-stage test results. The test results are shown in Table 1. One can see that the formulae of non-linear injury summation give a good description of the scattered injuries stage of corrosion cracking.

For the systems of metal-aggressive medium in which the operating life of the article is defined basically by the growth stage of a macroscopic crack it is advisable to use the damage mechanics method in the calculations on strength and durability. We propose the dependences to define the damage parameters on the basis of the well-known conceptions about the energy damage criteria as well as the dependence (Ford and Silverman, 1980; Takaku et al., 1979) of the type:

$$a = kt^m \quad (9)$$

where  $a$  - crack length,  $t$  - time,  $k$  and  $m$  - empirical coefficients. The dependences in which the damage parameters with the help of empirical coefficients are connected with the deformation rate are as follows:

$$t_p = Z \dot{\epsilon}^{-(n+1)/m} \quad (10)$$

$$\xi_p = Z \dot{\epsilon}^{m/M} \quad (11)$$

$$a_p = kZ \dot{\epsilon}^{-m(n+1)/M} \quad (12)$$

$$V_p = kZ \dot{\epsilon}^{m-1} \{ (1-m)(n+1) \} / M \quad (13)$$

where  $t_p$  - time before damage,  $\xi_p$  - relative length-ending at damage moment,  $a_p$  - crack length at damage moment,  $V_p$  - average crack growth rate,  $m, n, G, k$  - empirical coefficients,  $M = m + n + 1$ ;  $Z = (G/k)^{1/M}$ . Such an approach makes it possible to define the damage parameters proceeding from the results of the speeded up tests on corrosion cracking with constant deformation rate and to prognosticate the construction durability and strength taking into account the actual deformation rates of the order of  $10^{-8} - 10^{-9} \text{ sec}^{-1}$  characteristic to the operating of a number of the energy units equipment.

Table 1. Two-Stage Test Results of Steel Samples in 42% Solution  $\text{MgCl}_2$

$\sigma_{(1)}$ MPa	$\tau_1$ min	$t_1$ min	$\sigma_{(2)}$ MPa	$\tau_2$ min	$t_2$ min	Injury $\Pi$ by the formula					
						(1)	(3)	(4)	(5*)	(6)	(8)
12X18H12M3TЛ											
210	150	384	90	1440	3350	0.82	1.10	1.09	1.17	1.05	0.73
210	180	384	90	1080	3350	0.79	1.09	1.06	1.14	1.01	0.73
210	180	384	90	900	3350	0.74	1.02	1.05	1.09	0.99	0.69
90	1980	3350	210	40	384	0.70	0.79	0.88	0.99	1.09	0.72
90	1140	3350	210	78	384	0.54	0.64	0.81	0.91	0.95	0.75
90	1140	3350	210	80	384	0.58	0.65	0.81	0.94	0.96	0.77
210.5	120	380	101	780	2747	0.60	0.93	1.04	0.97	1.02	0.61
189.5	120	556	90.5	1500	3321	0.67	0.97	1.08	1.02	0.94	0.68
84.3	960	3714	175.8	90	712	0.39	0.56	0.77	0.77	0.72	0.59
90.5	960	3714	175.8	90	712	0.39	0.56	0.77	0.77	0.72	0.63
05X18AH6M2ФЛ											
210	180	679	90	1110	4338	0.52	1.05	1.03	0.95	1.09	0.41
210	240	679	90	180	4338	0.40	0.74	0.98	0.74	1.03	0.53
90	1800	4338	210	390	679	0.99	0.82	0.85	1.35	1.25	1.05
90	1320	4338	210	630	679	1.23	1.12	0.84	1.48	1.28	1.22
175.5	180	1158	75.5	690	5427	0.28	0.70	0.96	0.68	0.83	0.32
175.5	180	1158	75.5	1260	5427	0.39	0.81	0.99	0.81	0.87	0.42
189.5	187	932	90.5	780	4304	0.38	0.79	0.99	0.85	0.99	0.42
75.5	738	5427	167	660	1320	0.64	0.68	0.72	1.02	0.92	0.72
75.5	720	5427	167	318	1320	0.37	0.57	0.71	0.79	0.82	0.50

Table 2. Comparison of Experimental and Analytical Damage Parameters Values for 12X18H12M3T $\lambda$  (A), 05X18AH5 $\Phi$  $\lambda$  (B), 08X18H10T (C) Steels in 42% Solution of MgCl<sub>2</sub> and 25X15H7M2 (D) Steel in High Parameter Medium.

Steel Quality	Parameter	Deformation rate, sec <sup>-1</sup>				
		1.2 · 10 <sup>-4</sup>	10 <sup>-5</sup>	1.1 · 10 <sup>-6</sup>	0.9 · 10 <sup>-7</sup>	10 <sup>-8</sup>
A	t <sub>p</sub> (hours)	e 0.3	1.125	5.5	70	-
		a 0.21	1,309	6.719	42.9	218.6
	ε <sub>p</sub>	e 0.1	0.036	0.02	0.0182	-
		a 0.0898	0.047	0.027	0.0139	0.008
	a <sub>p</sub> (mm)	e 1.288	1.5	1.625	1.875	-
		a 1.297	1.464	1.63	1.841	2.05
V <sub>p</sub> (mm/sec)	e 1.19 · 10 <sup>-3</sup>	3.7 · 10 <sup>-4</sup>	8.2 · 10 <sup>-5</sup>	7.44 · 10 <sup>-6</sup>	-	
	a 1.7 · 10 <sup>-3</sup>	3.1 · 10 <sup>-4</sup>	6.7 · 10 <sup>-5</sup>	1.19 · 10 <sup>-5</sup>	2.6 · 10 <sup>-6</sup>	
B	t <sub>p</sub> (hours)	e 0.72	2.5	8.6	-	-
		a 0.68	2.43	7.5	26.9	82.3
	ε <sub>p</sub>	e 0.3	0.075	0.028	-	-
		a 0.296	0.087	0.03	0.0087	0.003
	a <sub>p</sub> (mm)	e 0.792	1.18	1.68	2.5	3.58
		a 0.792	1.18	1.7	-	-
V <sub>p</sub> (mm/sec)	e 3.1 · 10 <sup>-4</sup>	1.33 · 10 <sup>-4</sup>	5.65 · 10 <sup>-5</sup>	-	-	
	a 3.2 · 10 <sup>-4</sup>	1.35 · 10 <sup>-4</sup>	6.2 · 10 <sup>-5</sup>	2.6 · 10 <sup>-5</sup>	1.2 · 10 <sup>-5</sup>	
C	t <sub>p</sub> (hours)	e 0.61	3.1	7	58	-
		a 0.52	2.38	9.2	43	166
	ε <sub>p</sub>	e 0.222	0.0926	0.232	0.0152	-
		a 0.224	0.0857	0.0366	0.0139	0.006
	a <sub>p</sub> (mm)	e 0.475	0.68	1.125	1.425	-
		a 0.474	0.694	0.975	1.433	2.009
V <sub>p</sub> (mm/sec)	e 2.14 · 10 <sup>-4</sup>	6 · 10 <sup>-5</sup>	4.46 · 10 <sup>-5</sup>	6.82 · 10 <sup>-6</sup>	-	
	a 2.54 · 10 <sup>-4</sup>	8.1 · 10 <sup>-5</sup>	3 · 10 <sup>-5</sup>	9 · 10 <sup>-6</sup>	3.3 · 10 <sup>-6</sup>	
D	t <sub>p</sub> (hours)	e 0.65	11.58	72	380.5	-
		a 1.135	8	45.3	324	1822
	ε <sub>p</sub>	e 0.234	0.22	0.212	0.144	-
		a 0.49	0.288	0.18	0.105	0.07
	a <sub>p</sub> (mm)	e 0.438	0.795	0.776	0.972	-
		a 0.482	0.614	0.971	0.972	1.203
V <sub>p</sub> (mm/sec)	e 1.87 · 10 <sup>-4</sup>	1.69 · 10 <sup>-5</sup>	3 · 10 <sup>-6</sup>	7.1 · 10 <sup>-7</sup>	-	
	a 1.2 · 10 <sup>-4</sup>	2.1 · 10 <sup>-5</sup>	4.6 · 10 <sup>-6</sup>	8.3 · 10 <sup>-7</sup>	1.8 · 10 <sup>-7</sup>	

where e and a - experimental and analytical parameters values.

The experiment results and the analytical damage parameters values are shown in Table 2 where the correspondence of the analytical and experimental values is obvious. It is suggested that the construction elements calculation should be made with the help of complex approach. When the article requirements exclude crack formation it is advisable to evaluate its operating life according to the kinetic injury accumulation equations. For more massive or less important articles where some plastic deformation and the work at crack is acceptable it is advisable to use the equations based on damage mechanics principles.

The process description of multicycle fatigue scattered injuries is suggested to use the kinetic force-type equations. We have tested different equations and defined the efficiency of using the formulae of non-linear injury summation similar to the ones stated above for corrosion cracking with substitution of the time parameter by the cycle number.

As to the low-cycle fatigue processes two variants are acceptable, one of which is based on Coffin-Manson equation where constant coefficients are determined on the basis of low-cycle fatigue experiments. The disadvantages of this approach are the considerable duration and labour-intensiveness of the experimental determination of these coefficients.

To simplify the task we propose the following method. In the worst loading conditions in medium the characteristics of the material were determined according to the speeded up test results by constant deformation rate method. These characteristics were used for low-cycle fatigue description of the material to theoretical curve. Low-cycle fatigue curve equation for symmetrical cycle and strict loading regime is as follows:

$$e_a = \left(1/4N^{m_p}\right) \cdot \ln 1/(1-\psi_k^t) + \sigma_i^t/E^t \quad (14)$$

where  $m = 0.5$ ,  $\sigma_i^t = \sigma_s^t \cdot 0.4$  with  $\sigma_i^t < 700 \text{ MPa}$

Theoretical fatigue curve in the air for 10GH2M $\Phi$ A steel at 350°C determined from this equation is shown in Fig. (Curve 1).

As deformation ability is one of the principal values of the equation it is advisable to determine the theoretical low-cycle fatigue curve according to the speeded up test results for the metal-medium systems where corrosion-mechanical injury development takes place mainly according to electro-chemical mechanism. The minimum value of relative construction obtained at the test in aggressive medium with critical deformation rate value is used for this purpose. As shown in Fig. (Curve 2) such a theoretical curve is the envelope which bounds to its left the obtained experimental low-cycle fatigue data in the strict loading regime.

In view of brittle sample damage under the test with low deformation rate of the order of  $10^{-6}$  sec $^{-1}$  as well as damage moment which practically coincides with crack formation it can be supposed that the theoretical curve 2 (Fig.) corresponds to low-cycle crack formation moment. Test points obtained according to the well-known methods (Mazepa, 1989) correspond to the fatigue crack formation moment, these points being situated slightly to the right of theoretical curve 2 (Fig.). Such a good correspondence in the metal-medium system can be obviously explained by the fact that the process of corrosion-mechanical injury formation and development takes place mainly according to one and the same mechanism.

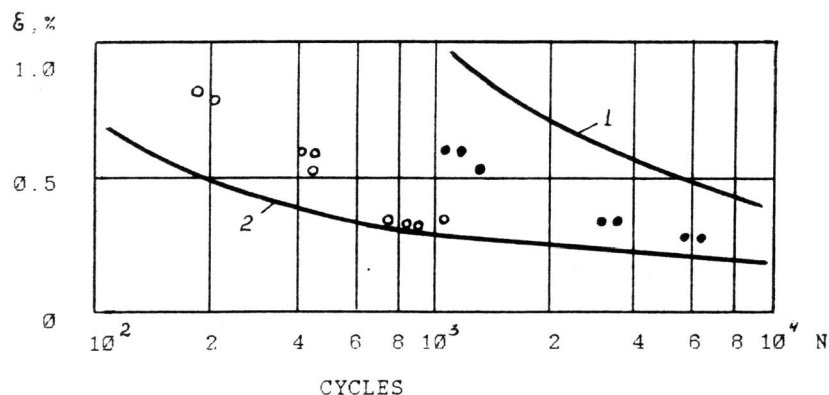


Fig. Low-cycle fatigue curves for 10 H2M A-steel

- 1 - theoretical fatigue curve in the air at 350°C;
- 2 - theoretical fatigue curve in the medium;
- - experimental low-cycle fatigue data according to rapture moment;
- - experimental data according to crack initiation moment.

#### REFERENCES

Ford F.P., Silverman M.J., 1980, Effect of loading rate on environmentally controlled cracking of sensitized 304 stainless steel in high purity water. *Corrosion*, v.36, pp.597-603.  
 Mazepa A.G., 1989, Low-cycle fatigue evaluation of alloys. *The Zavodskaya Laboratoriya*, v.55, N 10, pp.55-59. (in Russian)  
 Takaku h., Takiwai M., Hirano H., 1979, Crack growth behavior of type 304 stainless steel in oxygenated high temperature pure water. *Corrosion*, 35(11), pp. 523.

## MECHANISM OF THE EFFECT OF A MEDIUM ON SUBSTRUCTURE, MECHANICAL PROPERTIES AND FRACTURE OF SOLIDS

G.G. KOCHEGAROV

*Institute of Geophysics,  
 Siberian Branch of the Russian Academy of Sciences,  
 Universitetskij pr. 3, Novosibirsk, 630090, Russia*

#### ABSTRACT

The paper discusses mechanism of the effect of adsorbtionally-active medium (AAM) on fine crystal structure and mechanical properties of solids during dispersion. By the method of harmonic analysis of X-ray diffraction lines profile we investigated changes of crystal lattice microdistortions and domain of X-ray beams coherent scattering of the dispersed minerals and effect on AAM parameters under investigation. Mechanism of "scale strengthening" of solids during their dispersion is explained by strengthening of the surface layer of the dispersed particles. By lowering free surface energy of solids, AAM decreases the work of plastic deformation at their dispersion.

#### KEYWORDS

Solid, substructure, "scale strengthening", physical-mechanical properties, adsorbtionally-active medium, dispersion.

#### INVESTIGATION OF THE EFFECT OF THE MEDIUM ON SUBSTRUCTURE AND MECHANICAL PROPERTIES OF SOLIDS DURING THEIR DISPERSION

Physical-mechanical properties of solids are connected with the character of crystal structure defects, their distribution on the surface and in the volume of a solid. Dispersion of solids causes changing of the crystal structure (Kochegarov, 1986) and energetic state of the surface layer of the dispersion phase. Study of the substructural parameters - values of the crystal lattice microdistortions (M) and domain of X-ray coherent scattering (D) - was carried out by the method of harmonic analysis of X-ray diffraction lines profile (Kochegarov, 1978).

Dispersion of quartz was conducted in the air, in distilled water and water solutions of surface-active substances: cetyltrimethylammonium bromide (CTAB) of  $0,34 \cdot 10^{-4}$  -  $2,50 \cdot 10^{-4}$  mol/l concentration, hexylsulfuric sodium (HSS) of  $1,23 \cdot 10^{-4}$  -  $9,80 \cdot 10^{-4}$  mol/l concentration and OP-10 (polyethyleneether of mono- and dialkylphenols) of  $1,25 \cdot 10^{-2}$  -  $2,50 \cdot 10^{-3}$ % weight concentration. Parameters of the initial quartz substructure made up the values:  $M = 2,49 \cdot 10^{-4}$  and  $D = 810 \text{ \AA}$ .

The results of estimation of quartz substructure parameters

dispersed in various media are given in the table, which show, that quartz dispersed in the air undergoes more effective complication of the substructure, than that dispersed in water or in solutions of surface-active substances. Quartz dispersed in the air reveals more intensive development of microdistortions, than that dispersed in AAM. Relaxation of microdistortions is accompanied by D grinding, which proceeds more intensively during dispersion of quartz in the air, than in AAM.

Table: Effect of the medium on M and D values of dispersed quartz

Medium	M · 10 <sup>-4</sup>	D, Å
Air	14,0	300
Water	3,2	630
CTAB, HSS, OP-10	6,5-11,5	610-400

Increase of M value and of the substructural elements is limited by the area of localized highest stresses characterized by their rapid decrease in the area of the shear localization. Hence, the observed substructural complication of the dispersed quartz takes places, mainly, in the surface layer (1) of the particles (Kochegarov, 1988), which is deformed plastically during passing through the crack.

Analysis of literature data on kinetics of M and D development of dispersing apatite, cassiterite, kaolinite, lepidolite and chlorite as well as the data on changing the degree of apatite crystallinity and mica structure (see the figure) also shows, that dispersion of these minerals in the air causes more deeper structural changes of particles, than dispersion in water (Kochegarov, 1986). This may be explained, in our point of view, by following.

Localization of plastic deformation at dispersion of minerals in AAM causes lowering of the dispersion work as a result of the energy expense on their plastic deformation. Indeed, during brittle fracture of a solid the correlation is satisfied (Griffith):  $P = \text{const} \sqrt{E \sigma / c}$  (where P is the solid strength, E is Young's modulus, c is crack length,  $\sigma$  is free surface energy). During fracture, followed by plastic deformation, real work of formation of a new surface (effective surface energy  $G^*$ ) includes work of plastic deformation (w):  $G^* = G + w$  (Rehbinder and Shchukin). Experimental results obtained in this work shows, that AAM by lowering free surface energy of solids, simultaneously decreases the work of plastic deformation (w). As a result of this, the work of new surface formation  $G^*$  during dispersion of solids in AAM decreases and the dispersion process in AAM proceeds more intensively, than in the air.

During dispersion of solids, as linear size (L) of the dispersed particles decreases, specific consumptions of energy on their destruction increase, which is related to "scale strengthening", i.e. an increase of particles strength as their size decrease. Scale strengthening is explained by decreasing probability of finding "dangerous" crack in the particle,

which is likely, valid for threadlike monocrystals. However,

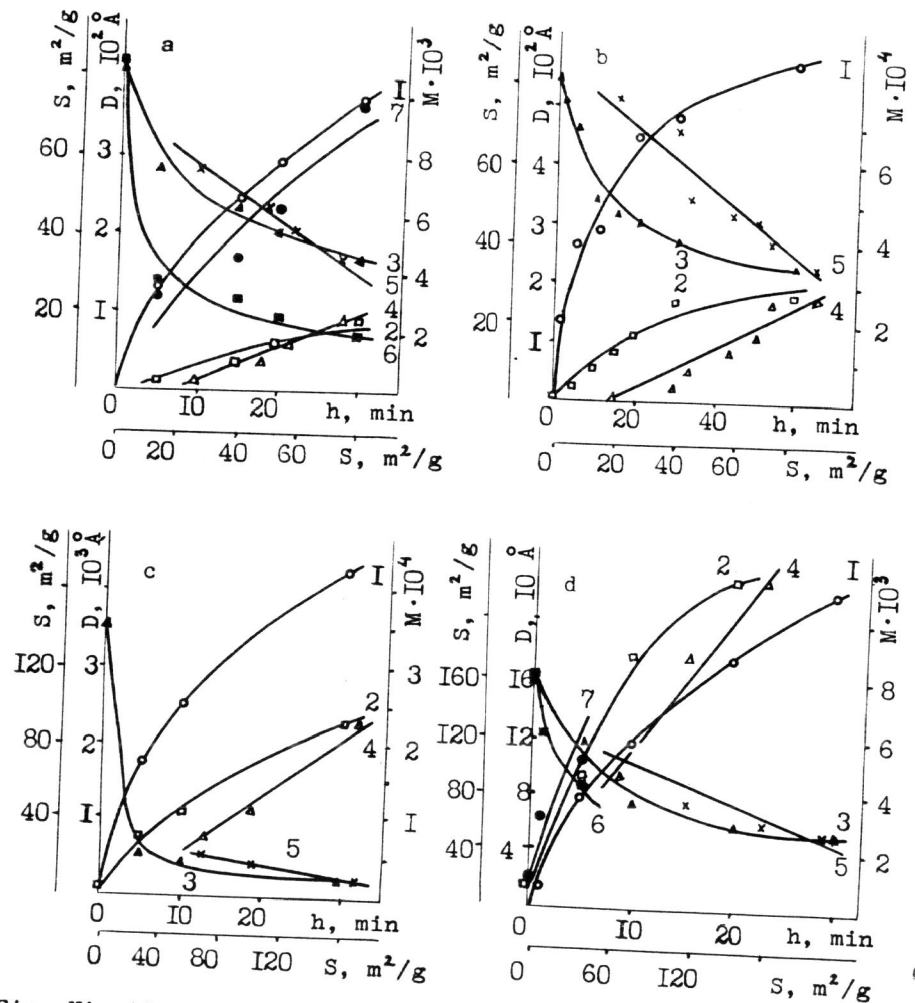


Fig. Kinetics of dispersing cassiterite (a), chlorite (c) and lepidolite (d) in water (1); kinetics of developing M of these minerals during dispersion in water (2) and in the air (7) and D during dispersion in water (3) and in the air (6); dependence of M (4) and D (5) values on the change of the degree of these mineral's dispersity.

as it is noted in (Chodakov, 1972), when dispersed, each particle is multiply subjected to stresses, close to maximum ones, which cause formation and development of new defects. Thus, it is unlikely that the density of defects changes distinctly, and the mechanism of scale strengthening remained obscure.

Increase of particle strength is explained by surface layer destruction with thickness "l". During dispersion of solids, when  $L \gg l$ , the fracture crack develops, mainly, along nonstrengthened domain of particles. Further, when "L" becomes comparable with "l", contribution of the strengthened layer into mechanical properties of the particle becomes noticeable. In the limiting case with  $L = 2l$  the particle strength increases to its maximum.

#### REFERENCES

1. Chodakov G.S. (1972), *Physika Izmelcheniya*. Nauka. Moskow. (in Russian).
2. Griffith A.A. (1920), *The Phenomena of Rupture and Flow in Solids*. Trans. Phil. Roy. Soc. Vol. 221A. P. 163-198
3. Kochegarov G.G. (1978), Estimation of Characteristics of the Thin of Crystalline Structure Dispersed Quartz by Harmonic Analysis Method. *Izvestiya SO AN SSSR. Ser. Chim. Nauk. Vip. 5. N. 12. P. 65-70.* (in Russian).
4. Kochegarov G.G. (1986), Destruction of the Mechanically Activated Solids. *Izvestiya SO AN SSSR. Ser. Chim. Nauk. Vip. 1. N. 2. P. 65-71.* (in Russian).
5. Kochegarov G.G. (1988), Change of Structure and Mechanical Properties of Mineral Substances During Dispersion. *Izvestiya AN SSSR. Neorganicheskie materialy. T. 24. N. 1. P. 73-76.* (in Russian).
6. Rehbinder P.A. and Shchukin E.D. (1972), Surface Phenomena of Solids in Processes Their Deformation and Rupture. In: *Progress in Surface Science* (Ed. by S.Davison). Vol. 3. Pt. 2. P. 97-153. Pergamon Press. Oxford.